ISSN 0511-5728
The West Indian Journal of Engineering
Vol.45, No.1, July 2022, pp.39-49

Measurement of Swash Infiltration Rates on Sandy Beaches

Shani Brathwaite [a] and Deborah Villarroel-Lamb [b,Ψ]

Department of Civil and Environmental Engineering, Faculty of Engineering, The University of the West Indies, St. Augustine, Trinidad and Tobago, West Indies;

[a]Email: shani_brathwaite@hotmail.com
[b] Email: Deborah.Villarroel-Lamb @sta.uwi.edu

[Ψ] *Corresponding Author*

(Received 09 August 2021; Revised 28 May 2022; Accepted 07 June 2022)

Abstract: *The swash zone is a critical area of the nearshore hydrodynamics contributing significantly to beach evolution. The role of infiltration of water during swash events has been investigated, but an enhanced data collection methodology will improve prediction and analyses of swash processes. A new and simple technique was proposed to determine the rate of swash infiltration on sandy beaches. Direct, in situ measurements of swash infiltration rates were conducted on the sandy beach of Las Cuevas Bay located on the north coast of Trinidad. The method incorporated the use of a double ring infiltrometer paired with a Bluetooth water level logger, where infiltration rates were inferred from the changes in water level recorded within the double ring infiltrometer. Observed infiltration rates were variable and showed a dependency on sediment characteristics and location of measurement. The study also sought to ascertain any correlation between the measured infiltration rates and sediment properties. While correlation was generally low, the use of the maximum recorded infiltration rate yielded the best correlation across most cases observed. In addition, the highest correlation occurred with the* D_{10} *grain size for the upper beach, and the* D_{90} *grain size for the lower beach which is closer to the Still Water Line. The sediment sorting ratio of* D_{84}/D_{16} *and* D_{90}/D_{10} *showed the best correlation for the upper and lower beach locations respectively. While the field method was practical, the results of the study demonstrate a need to capture additional bed features that contribute to the rate of infiltration.*

Keywords: *Swash zone; infiltration; sandy beaches; in situ measurement; grain size; infiltrometer*

1. Introduction

Swash infiltration is the downward flow of water into the beach face during the run-up and run-down of a swash event (Turner and Masselink, 1998). The rate at which the water moves through the sand is affected by the height of the water table, as well as, the physical and biochemical properties of the individual particles such as its shape, angularity and size (Horn, 2002). Beaches with lower water tables are defined as dry foreshore beaches that incur faster rates of infiltration (Grant, 1946). According to Bakhtyar et al. (2009) and Sous et al. (2016), infiltration is more likely to occur in the uppermost part of the beach under coarse grain conditions. For fine to medium grain type beaches, the percolating swash interacts with air pressure below the surface inhibiting infiltration processes. However, in the case of gravel beaches, the buildup of pressure below the surface is weaker and infiltration readily occurs (Steenhauer et al., 2012).

Research has shown that swash infiltration plays a significant role in the maximum positions of wave run-up and sediment transport in the swash zone (Masselink and Li, 2001; Nielsen and Hanslow, 1991). The loss of water through percolation reduces the volume and velocity of the swash lens, resulting in lower limits of wave run-up, as well as, the accompanying sediment deposition. The reduced volume and velocity of the swash lens weaken the backwash, reducing the chances of sediment transport down the foreshore slope (Horn, 2002).

A large percentage of data on infiltration in the swash zone has been obtained from the observation of ground water table fluctuations (Nielsen et al., 2001). An early attempt at the direct observation of infiltration processes in the swash zone was recorded by Turner and Masselink (1998). A pair of high sensitivity pressure sensors, fixed 150mm apart onto an aluminum frame, were buried vertically such that the top sensor was always between fifteen (15) and five (5) mm below the surface. Using Darcy's law, the infiltration rates occurring per swash event were derived from the vertical pore-pressure gradient between the two buried sensors and estimated values of hydraulic conductivity using the equation by Krumbein and Monk (1942). However, this equation by Krumbein and Monk (1942) has since been modified to account for the variation in porosity by Berg (1970) through a semi-theoretical/empirical method. Similarly, Butt et al. (2001) also attempted direct measurement of water percolation velocities within the beach face using miniature Druck PDCR830 pressure transducers. The accuracy of the pressure transducers was published as ±0.1%. The pore-pressure gradient between the top and

https://doi.org/10.47412/PPJX1408

bottom sensors was calculated assuming the flow was Darcian.

Austin and Masselink (2006) conducted an experiment on a steep, gravel beach to assess the exchange of water between swash lens and ground water in the swash zone. Five (5) pairs of miniature pressure transducers were deployed along a cross-shore transect. Each pair was arranged such that one (1) pressure transducer was deployed level with the bed to measure swash depths and the corresponding pressure transducer installed 0.75m below to determine water table positions. Two mini Valeport electromagnetic current meters were also installed to record flow velocities. They were placed 0.03m from the bed above the two most seaward pairs of pressure transducers. Infiltration and exfiltration were measured using the instantaneous swash flux as a substitute. The swash flux, Q, was calculated as the product of the instantaneous water depth and the velocity at each time step. However, using the electromagnetic current meter it is impossible to separate the horizontal and vertical velocities during a swash event and as such presented a limitation in this method of estimation.

Sous et al. (2016) also conducted a study on the groundwater swash zone using a network of five (5) vertical poles each equipped with three (3) pressure transducers equidistant apart. The transducers measured relative pressure and were time-synchronised, logging at a sampling rate of 10Hz. The velocity of the water flow was estimated using Darcy's law, and the hydraulic conductivity was estimated from a series of falling head test conducted on sediment samples taken from the study area.

Hamada et al. (2018) determined the rate of infiltration on a lakeshore beach by measuring the residue of a tracer injected into transparent cylinders buried in sand. The cylinders were filled with a slurry of a water-sand mixture and sealed at both ends with nylon nets (100-µm mesh). Fifty (50) mm of a water and sodium fluorescein solution (the tracer) was poured into the cylinders and buried vertically 5cm below the surface and observed for a period of 5-30 minutes. The remaining tracer at the end of the observation period was flushed out using 50ml of pure water and its concentration determined by a portable data logging colorimeter (DR/820, Hach) set at a 470-nm wavelength. This technique used by Hamada et al. (2018) is limited to sandy layers.

Most recently, Gilfedder et al. (2021) installed five (5) temperature profiles along a cross-shore transect on a high energy, mesotidal beach to quantify and map infiltration and exfiltration zones. The temperature profiles consisted of eight (8) high sensitivity thermistors housed in a pointed stainless-steel tube at intervals of 0.08 m, 0.15 m, 0.37 m, 0.57 m, 0.78 m, 0.96 m, 1.16 m and 1.37 m. While attached to a circuit board, the resistivity of each sensor was measured and converted to temperature values, and then transmitted to a router via a RF24 chip. Using mobile data, the router sent the data to servers at the University of Bayreuth. Heat transport calculations from three solutions to the 1D heat transport equation, including 1) a steady state analytical solution, 2) a non-steady state numerical model, and 3) a non-steady state analytical solution, were used to quantify water flows. However, this technique used by Gilfedder et al. (2021) is heavily dependent on a vast difference in temperature between seawater and ground water.

In another research study by Seidel (1991) a double ring infiltrometer with diameters twelve (12) and twenty-four (24) inches was used to test the rates of infiltration in a model beach experiment. The rings were coupled with two (2) manometers and nozzles each connected to a reservoir. Both rings were driven where the central vertical axis was perpendicular into the soil. The reservoirs were then mounted above the rings to ensure that flow to the rings was gravity driven (see Figure 1). The time was then recorded at pre-determined levels in the reservoir as the water infiltrated into the bed. Infiltration rates were reported to increase by 33% for lower water tables. This technique provided a more direct measurement of infiltration rates. The main objective of this paper is to propose a similar direct method to observe swash infiltration on sandy beaches with a less cumbersome assembly of apparatus. Subsequently, the collected data will be used to perform a preliminary investigation of the factors influencing infiltration rate magnitudes.

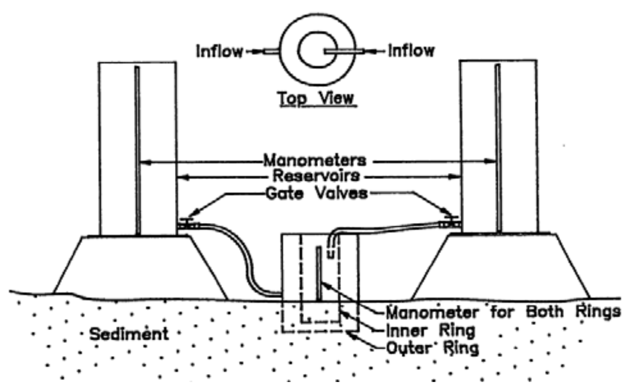

Figure 1. Schematic of Infiltrometer (Seidel 1991)

2. Methodology

2.1 Study Site Description

This study was conducted at Las Cuevas Bay, a micro-tidal beach located on the northern coast of Trinidad (see Figure 2). Las Cuevas Bay is approximately 2.2 km long bounded by two prominent headlands on its western and eastern ends. Waves within the bay approach the coastline, predominantly from the north, as rows of plunging breakers with an average wave height of about 0.15m and a wave period of 9.08s. The beach is gently sloping and comprises of sediment which can be classified as slightly gravelly sand with a mean grain size of 0.19mm

(Darsan et al., 2012; Institute of Marine Affairs (IMA), 2013).

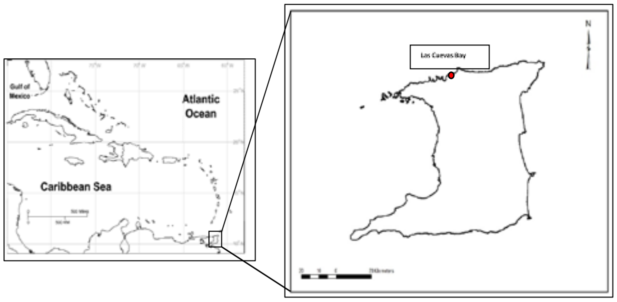

Figure 2. Map Illustrating the Study Site Location

2.2 Instrumentation

A double ring infiltrometer paired with a water level logger was proposed for the measurement of swash infiltration rates. The double ring infiltrometer is a simple instrument used to determine actual field measurements of water infiltration rates through soil. The instrument consists of one pair of stainless steel rings measuring twelve (12) inches and twenty-four (24) inches in diameter and twenty (20) inches in length. It also comprises of a measuring bridge and measuring rod with float.

In order to facilitate the anticipated fast infiltration rates and the associated high probability of observation errors, the measuring rod was replaced with a water level logger. For the purpose of this research, the MX2001-04 water level logger was selected (see example in Figure 3).

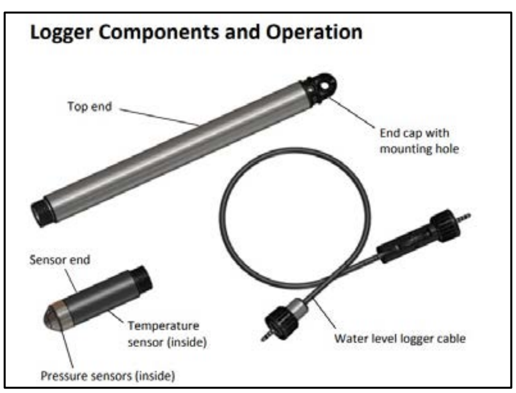

Figure 3. Bluetooth water level logger used to observe the water level within the double ring infiltrometer as it infiltrates through the beach face

The logger has an operation range from 0.0m to approximately 4.0m of water depth, at sea level, with a resolution of 0.14cm. The typical water level accuracy of the logger is ±0.075% FS (Full Scale) (about 0.3cm) and may exhibit a maximum error of ±0.15% FS (about 0.6cm). The blue tooth device facilitates wireless communication with any mobile device compatible with the HOBOmobile 1.4 or later software. This device setup is simpler and easier to use when compared to the more cumbersome setup requiring an attachment of long wires and tubes. As such, it allows for a practical and ideal solution for field studies of water level changes in the dynamic swash zone.

2.3 Instrument Measurement Validation

Validation of the measurements from the instrument was conducted in a wave flume measuring 0.96m high, 0.55m wide and 10m long. One side panel of the wave flume was labelled at 5cm increments from its base, and the flume was filled to a depth of 55cm with fresh water. The water level logger was then strapped to a length of polyvinyl chloride (PVC) and submerged near the base of the flume. The flume was then allowed to be emptied, and the time the water level arrived at each 5cm increment was observed and noted. From the data downloaded from the water level logger, the change in water level over each recorded time increment was calculated. The percentage errors in the readings of the water level logger were calculated where a positive error value represented a measured water level change greater than expected.

2.4 In Situ Testing

For the field testing, infiltration measurements were conducted at two positions along the cross shore of the beach: Position A located approximately one (1) meter from the landward extent of the area being repeatedly wetted, and Position B located in the dry upper beach. Position A was on the lower beach area closer to the Still Water Line (SWL). Measurements were done along four (4) transect lines within Las Cuevas Bay; therefore the rate of infiltration was measured at eight (8) points on the coast. Four (4) of those points were located just beyond the maximum point of wave run-up (in the lower beach) and four (4) were collected on the dry upper beach. A schematic diagram of the transect line, L1, is presented in Figure 4.

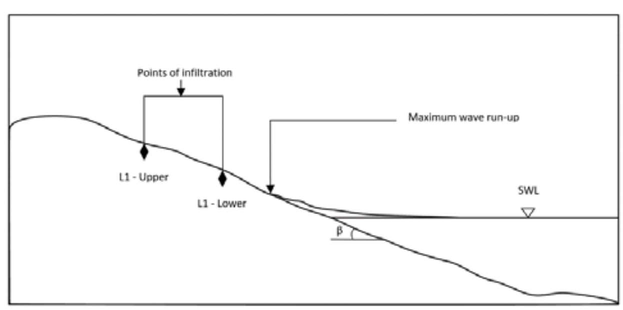

Figure 4. Schematic Diagram of Infiltration Rates at Upper and Lower Points along Transect Line L1

The rings were inserted 10 cm into the beach face and a support arm for the water level logger positioned within the inner ring. The data logger was configured using the HOBOmobile software on a mobile device, setting the reference level to zero and the logging interval set to one reading every second (i.e. a sampling frequency of 1Hz). The double ring infiltrometer was then filled with sea water. However, in order to ensure a vertical flow of water through the measuring ring, the buffer ring was filled first.

The water level logger was strapped to a length of PVC suspended from the support arm such that the pressure transducer was approximately two (2) cm from the beach face. Measurements were taken until the water level within the inner ring completely drained. Figure 5 illustrates the experimental set-up on the dry upper beach. Infiltration rates were calculated using the absolute value of the change in water level recorded by the water level logger for each minute, over the first five (5) minutes of data collected. This analysis yielded five (5) data points for the infiltration rate at each of the eight (8) locations. Using these five (5) values, the averaged, maximum and minimum infiltration rates were recorded for each location.

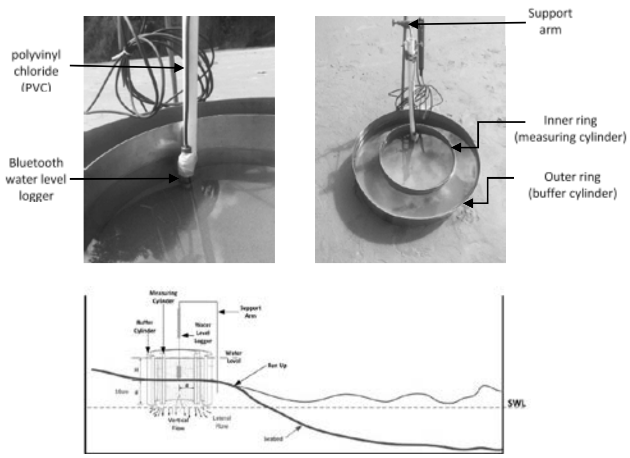

Figure 5. Deployment of Double Ring Infiltrometer Paired with the Bluetooth Water Level Logger

2.5 Grain Size Analyses

Sediment samples were collected at each of the eight locations where the infiltration rates were observed, and a sieve analysis was conducted to determine the grain size distribution. This analysis sought to identify the representative grain size which would show the greatest correlation with the infiltration rates. Therefore, the D_{10}, D_{50}, and D_{90} grain sizes were extracted from the grain size distribution. The correlation between the infiltration rates and the various grain sizes was used as a means to identify the representative grain size parameter that will likely control the infiltration rates. Additionally, the role that sediment gradation or sorting played in the infiltration was also investigated. Sediment sorting ratios of D_{90}/D_{10}, D_{75}/D_{25} and D_{84}/D_{16} were also extracted from the grain size distribution analyses and any correlation with the infiltration rate was investigated. The GRADISTAT tool, which is a grain size distribution and statistics package, was used to facilitate the sediment gradation analyses (Blott and Pye, 2001).

3. Results and Discussion

The proposed technique to measure swash infiltration rates was successfully validated in the laboratory, and then testing executed in the field on a sandy microtidal beach. The results of the validation exercise conducted in the laboratory flume are shown in Table 1. An averaged percentage error of negative one (1) percent was determined from these experiments. This result indicates a tendency of the instrument to slightly underestimate the infiltration rates. However, possible errors associated with the validation process may arise from the delay in observing the water level, and recording the time at that instant. Nonetheless, these validation results demonstrate that the methodology can yield meaningful results of water level changes over time, and within the range of expected error of the instrument.

As anticipated for the in situ study, the apparatus was simple to assemble in the field and was void of any cumbersome wires. The technique allowed for direct, in situ measurement of swash infiltration rates with minimal disturbance to the beach face, and the Bluetooth capabilities allowed for quick data retrieval from the mobile device. The minimum time for the water to completely infiltrate the dry beach face was approximately five (5) minutes for the eight (8) positions on Las Cuevas beach. The results of the field tests are presented in Table 2 and Figure 6.

Table 1. Validation of Test Results

Time (hh:mm:ss)	Measured Depth taken from logger (ft.)	Measured Change in depth (ft.)	Measured Change in depth (cm)	Actual Change in depth (cm)	Error (%)
03:12:14	-0.152				
03:14:53	-0.32	0.168	5.12	5.00	2.4
03:17:03	-0.478	0.158	4.82	5.00	-3.7
03:19:16	-0.64	0.162	4.94	5.00	-1.2
03:21:34	-0.803	0.163	4.97	5.00	-0.6
03:23:51	-0.965	0.162	4.94	5.00	-1.2
03:26:20	-1.126	0.161	4.91	5.00	-1.9
03:28:00	-1.285	0.159	4.85	5.00	-3.1
03:31:48	-1.446	0.161	4.91	5.00	-1.9
03:35:04	-1.613	0.167	5.09	5.00	1.8
				Average Error	**-1.0**

Table 2. In Situ Results for Infiltration Rates on Las Cuevas Beach

Beach	Location	D_{10} (mm)	D_{50} (mm)	D_{90} (mm)	D_{90}/D_{10}	D_{75}/D_{25}	D_{84}/D_{16}	Averaged Infiltration Rate (cm/min)	Maximum Infiltration Rate (cm/min)	Minimum Infiltration Rate (cm/min)
Las Cuevas	L1 - upper	0.1324	0.1754	0.2398	1.8114	1.4479	1.6562	1.4113	1.9267	0.6944
	L2 - upper	0.1661	0.2523	0.5369	3.2321	1.7595	2.4475	1.6416	1.9960	1.3010
	L3 - upper	0.2649	0.3963	0.6061	2.2881	1.5650	1.9490	1.0804	1.2477	0.8993
	L4 - upper	0.1650	0.2663	0.3729	2.2605	1.5529	1.8422	1.0920	1.6990	0.6997
	L1 - lower	0.0966	0.1309	0.1790	1.8535	1.4713	1.6899	0.5408	1.6212	0.0163
	L2 - lower	0.1322	0.1760	0.2473	1.8701	1.4763	1.7013	0.7774	1.4437	0.3174
	L3 - lower	0.1546	0.2205	0.3204	2.0716	1.4034	1.6901	0.7116	1.1539	0.4511
	L4 - lower	0.2566	0.4097	0.5535	2.1575	1.3184	1.6780	0.7321	1.2656	0.2970

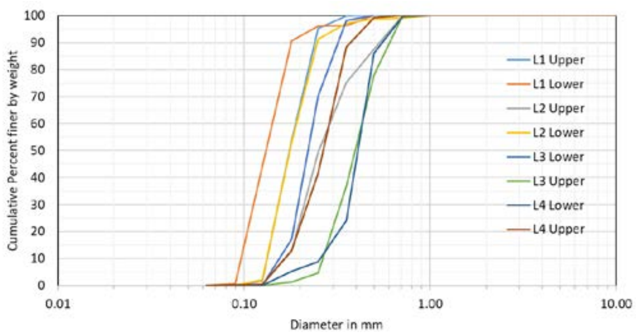

Figure 6. The Sediment Size Distribution for All the Samples

Table 2 shows the averaged, maximum and minimum infiltration rates at the eight (8) locations, disaggregated into Upper Beach and Lower Beach locations. The magnitude only is provided, but the flow of water is in a downward direction into the bed, for all cases. This direction of flow confirms that infiltration occurs as the swash lens progresses on to the dry upper beach. Table 2 also shows the associated grain sizes: D_{10}, D_{50}, and D_{90} at each of the eight (8) locations, as well as, the sediment sorting ratios of D_{90}/D_{10}, D_{75}/D_{25} and D_{84}/D_{16}.

Appendix 1 depicts plots of the averaged, maximum and minimum measured infiltration rates versus various grain sizes (mm) and sediment sorting ratios, respectively, for both Upper Beach and Lower Beach locations. Table 3 summarises the correlation coefficients, given as R^2 values, between the various sediment grain sizes or sorting ratios and the infiltration rates. The sediment sizes did not vary considerably for all the sediment tests, with the D_{10} sediment size showing the least variability. There was more variability within the D_{90} sediment size and consequently the D_{90}/D_{10} sediment sorting ratio. In spite of this, the variability observed in the infiltration rates was significant, with rates being much lower at the lower beach locations than at the upper beach locations. This result is consistent with the observations of other researchers (Bakhtyar et al., 2009; Grant, 1946; Horn, 2002), and clearly alludes to the influence of other factors, such as the water table elevation and degree of wetness of the sediment, in the infiltration rates expected in the swash zone.

Observed trends with this measured dataset showed that the representative sediment size did impact the infiltration rate. The magnitude and type of effect observed depended on the representative grain size used, as well as, the statistical value of the infiltration rate. If the averaged infiltration rates were used, the observed trend was a decreasing infiltration rate with increasing grain size in the upper beach locations, but an increasing infiltration rate with increasing grain size in the lower beach locations. Using the maximum observed infiltration rates, the observed trend was a decreasing infiltration rate with increasing grain size in both the upper and lower beach locations.

Using the minimum observed infiltration rates, the observed trend was an increasing infiltration rate with

Table 3. Correlation between Infiltration Rates and Sediment Size or Sorting Ratio

	Correlation given as an R^2 value						
	D_{10}	D_{50}	D_{90}	D_{90}/D_{10}	D_{75}/D_{25}	D_{84}/D_{16}	$(D_{84}/D_{16})^{1/2}$
	Upper Beach Locations						
Infiltration Rate							
Averaged	0.3013	0.3426	0.0076	0.3143	0.2762	0.3355	0.3095
Maximum	0.8443	0.8176	0.3009	0.0731	0.0517	0.0539	0.0431
Minimum	0.0215	0.0275	0.4394	0.8948	0.8884	0.9504	0.9433
	Lower Beach Locations						
Infiltration Rate							
Averaged	0.2656	0.2095	0.2350	0.1609	0.1032	0.0285	0.0282
Maximum	0.4058	0.3660	0.4243	0.7168	0.4729	0.1216	0.1217
Minimum	0.1904	0.1465	0.1880	0.3436	0.1582	0.0024	0.0023

increasing grain size for both the upper and lower beach locations. While correlation was generally low across all cases tested, the best correlation was observed mostly with the maximum infiltration rate, although in the upper beach locations there was some deviation from this general trend. For lower beach locations, the maximum infiltration rate yielded the highest correlations using the D_{10}, D_{50} and D_{90} sediment sizes with the highest observed value (R^2 = 0.4243) associated with the D_{90} grain size. This suggests that the maximum infiltration rate on the lower beach is controlled by the larger sediment sizes, but the poor correlation indicates that other factors contribute to the rate of infiltration. For upper beach locations, the maximum infiltration rate yielded the highest correlations using the D_{10} and D_{50} sediment sizes with the highest observed value (R^2 = 0.8443) associated with the D_{10} grain size. It may be inferred from these preliminary results that the smaller sediment grain sizes regulate the maximum infiltration rates in the upper beach and appears to be a dominant factor. The D_{90} does not appear to be as significant in the upper beach regions as correlations with the maximum and minimum infiltration rates were of the same order of magnitude and about half that observed with the D_{10} sediment size.

Observed trends between the sediment sorting ratios and the infiltration rates were also noted. In the lower beach regions, the trends for the D_{90}/D_{10}, D_{75}/D_{25}, D_{84}/D_{16} and $(D_{84}/D_{16})^{1/2}$ sediment sorting ratios mirrored those observed for the sediment sizes with respect to the maximum, minimum and averaged infiltration rates where the highest correlations were seen with the maximum infiltration rate, and the correlations with the minimum and averaged infiltration rates were much smaller. Generally, correlations were low for the lower beach areas, but the best correlation was observed with the maximum infiltration rates, where the D_{90}/D_{10} sorting ratio provided the highest correlation (R^2 = 0.7168).

In the upper beach regions, the trends for the D_{90}/D_{10}, D_{75}/D_{25}, D_{84}/D_{16} and $(D_{84}/D_{16})^{1/2}$ sediment sorting ratios did not imitate those observed for the sediment sizes with respect to the maximum, minimum and averaged infiltration rates. The highest correlations were seen with the minimum infiltration rate, where the correlations with the averaged infiltration rates were much smaller, and those associated with the maximum infiltration rate were near zero.

In the upper beach areas for the minimum infiltration rates, correlations were quite high with the highest correlation being observed with the D_{84}/D_{16} sorting ratio (R^2 = 0.9504), but where the correlations with all the sediment ratios for the minimum infiltration rates were on the same order of magnitude. Again, emphasising that these are preliminary results, it appears that the sediment size range is a dominant factor for the minimum infiltration rates in upper regions and any suitable sediment sorting ratio would be able to represent the sediment size gradation. The degree of sediment sorting does not appear to impact the maximum infiltration rates, and only has a minor role for the averaged infiltration rates.

For the lower beach, sediment sorting does not appear to be as a significant factor as seen in the upper beach. However, the D_{90}/D_{10} sediment ratio appears to be best able to capture any variability in these lower beach areas.

By inference, where low correlation scores are obtained, it emphasises the role of other factors in the infiltration rate, that is other than sediment size and grain size distribution. Even so, the maximum infiltration rate appears to be most dependent on the sediment size characteristics overall. This is true for both the sediment size and sorting features in the lower beach, but only true for sediment size in the upper beach.

There were a limited number of samples in this study and a greater number of samples at diverse locations should yield a wider range of sediment characteristics, from which a more rigorous analysis may be executed. There is also the need to investigate different approaches to estimating the infiltration rate from the water level logger. The study however, does show the methodology is adequate for measuring infiltration rates on sandy beaches. It is uncertain how the instrument will perform on mixed and gravel beaches which are expected to incur faster rates of infiltration. Therefore, further research is required to determine its applicability on mixed and gravel beaches.

4. Conclusion

This study tested a new and simple technique to obtain in situ infiltration rates within the swash zone of sandy beaches. Infiltration rates were measured using the change in water level observed using a Bluetooth water level logger over a given time. Infiltration rates varied considerably, with faster infiltration rates occurring on the dry upper beach. Using the data obtained, a relationship appears to exist between infiltration rate and sediment size, as well as, the sediment size distribution. Using the sediment sizes, the greatest correlation occurred with the maximum infiltration rates observed, and with the D_{10} and D_{90} grain sizes for the upper beach and the lower beach respectively. The sediment sorting ratio of D_{90}/D_{10} showed the best overall correlation for both the upper and lower beach locations, but a slightly higher correlation was observed with the D_{84}/D_{16} ratio for the upper beach. While more samples are required to improve trends between parameters, the study demonstrates that the measurement technique is suitable and can be readily integrated into a data collection exercise to improve the understanding of the processes within the swash zone.

References:

Austin, M. J. and Masselink, G. (2006), "Infiltration and exfiltration on a steep gravel beach: implications for sediment transport", in: *Coastal Dynamics 2005: State of the Practice*, pp.1-14.

Bakhtyar, R., Barry, D.A., Li, L., Jeng, D.S. and Yeganeh-Bakhtiary, A. (2009), "Modelling sediment transport in the swash zone: A review", *Ocean Engineering*, Vol.36, Nos.9-10, pp. 767-

783.

Berg, R.R. (1970), "Method for determining permeability from reservoir rock properties", *Gulf Coast Association of Geological Societies Transactions*, Vol.20, pp.303 - 317.

Blott, S.J. and Pye, K. (2001), "GRADISTAT: A grain size distribution and statistics package for the analysis of unconsolidated sediments", *Earth Surface Processes and Landforms*, Vol.26, No.11, pp.1237-1248.

Butt, T., Russell, P. and Turner, I. (2001), "The influence of swash infiltration–exfiltration on beach face sediment transport: Onshore or offshore?", *Coastal Engineering*, Vol.42, No.1, pp.35-52.

Darsan, J., Ramnath, S. and Alexis, C. (2012), *Status of beaches and bays in Trinidad 2004–2008*, Technical Report Institute of Marine Affairs, Trinidad.

Gilfedder, B.S., Waska, H., Wismeth, F. and Frei, S. (2021), "Using heat as a tracer to map and quantify water infiltration and exfiltration along a complex high energy beach face", *Estuarine, Coastal and Shelf Science*, Vol.250, pp.107140.

Grant, U.S. (1946), "Effects of groundwater table on beach erosion", *Geological Society American Bulletin*, Vol.57, pp.1952 (abstract).

Hamada, A., Nakamura, K. and Sasaki, K. (2018), "Simple estimate of filtration rates on a sandy beach", *Limnology*, Vol.19, No.1, pp.69-80.

Horn, D.P. (2002), "Beach groundwater dynamics", *Geomorphology*, Vol.48, Nos.1-3, pp.121-146.

IMA (2013), *A Guide to Beaches and Bays of Trinidad and Tobago*, 2nd Edition, Institute of Marine Affairs, Trinidad and Tobago

Krumbein, W.C. and Monk, G.D. (1942), "Permeability as a function of the size parameters of unconsolidated sand", *AIME Technical Publications (ZDB-ID 2589 114)*, Vol.1492, pp.153 - 163.

Masselink, G. and Li, L. (2001), "The role of swash infiltration in determining the beachface gradient: a numerical study", *Marine Geology*, Vol.176, Nos.1-4, pp.139-156.

Nielsen, P. and Hanslow, D. J. (1991), "Wave runup distributions on natural beaches", *Journal of Coastal Research*, Vol. 7, No. 4, pp.1139-1152.

Nielsen, P., Robert, S., Møller-Christiansen, B. and Oliva, P. (2001), "Infiltration effects on sediment mobility under waves", *Coastal Engineering*, Vol.42, No.2, pp.105-114.

Seidel, G.S. (1991), *An Experimental Investigation of the Effects of Tides on Subsurface Drains Used for Beach Stabilisation*, MSc Thesis, Lehigh University, Bethlehem, PA, USA.

Sous, D., Petitjean, L., Bouchette, F., Rey, V., Meulé, S., Sabatier, F. and Martins, K. (2016), "Field evidence of swash groundwater circulation in the Microtidal Rousty Beach, France", *Advances in Water Resources*, Vol.97, pp.144-155.

Steenhauer, K., Pokrajac, D. and O'Donoghue, T. (2012), "Numerical model of swash motion and air entrapment within coarse-grained beaches", *Coastal Engineering*, Vol.64, pp.113-126.

Turner, I.L. and Masselink, G. (1998), "Swash infiltration-exfiltration and sediment transport", *Journal of Geophysical Research: Oceans*, Vol.103, No.C13, pp.30813-30824.

Acknowledgments

The authors acknowledge the support of Campus Research and Publication Fund for their contribution to this research work.

Appendix 1. Plots of the averaged, maximum and minimum measured infiltration rates

- Figures 7 to 9 show plots of the averaged, maximum and minimum measured infiltration rates (cm/min) versus the D_{10}, D_{50}, and D_{90} grain sizes (mm) for the Upper Beach and Lower Beach locations.
- Figures 10 to 12 show plots of the averaged, maximum and minimum measured infiltration rates (cm/min) versus the D_{90}/D_{10} and D_{75}/D_{25} sediment sorting ratios, for the Upper Beach and Lower Beach locations.
- Figures 13 to 15 show plots of the averaged, maximum and minimum measured infiltration rates (cm/min) versus the D_{84}/D_{16} and $(D_{84}/D_{16})^{1/2}$ sediment sorting ratios, also for the Upper Beach and Lower Beach locations.

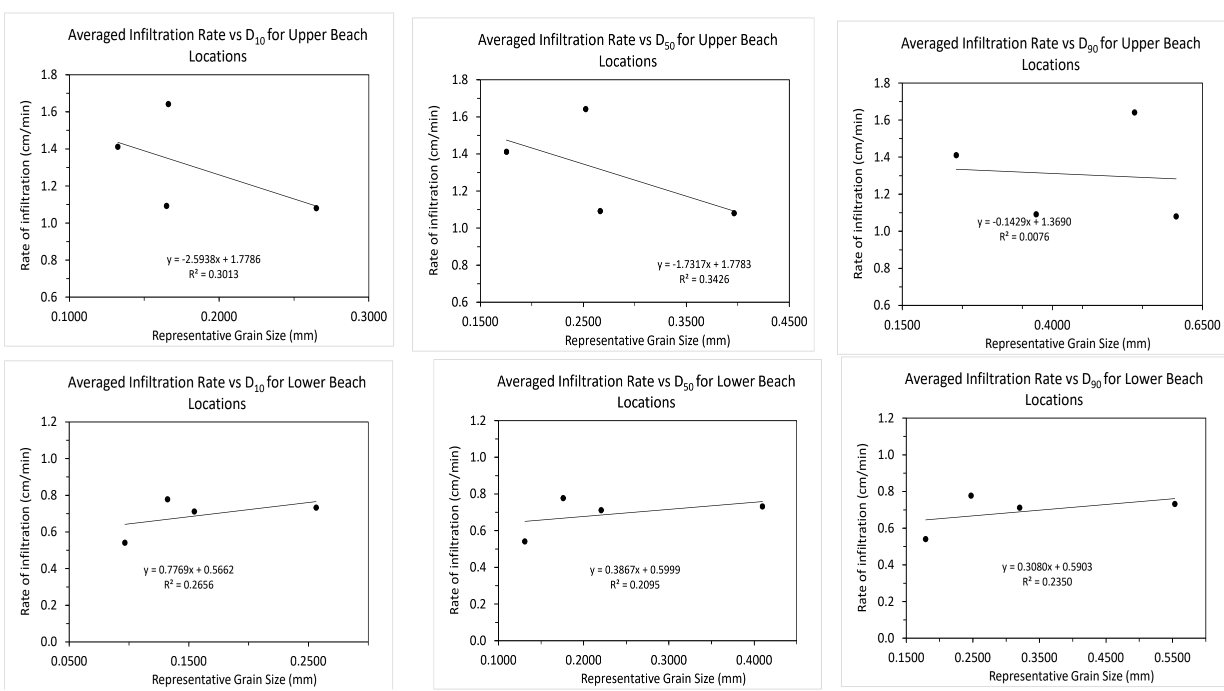

Figure 7. The Relationship between the D_{10}, D_{50}, and D_{90} Grain Sizes and the Average Rate of Infiltration

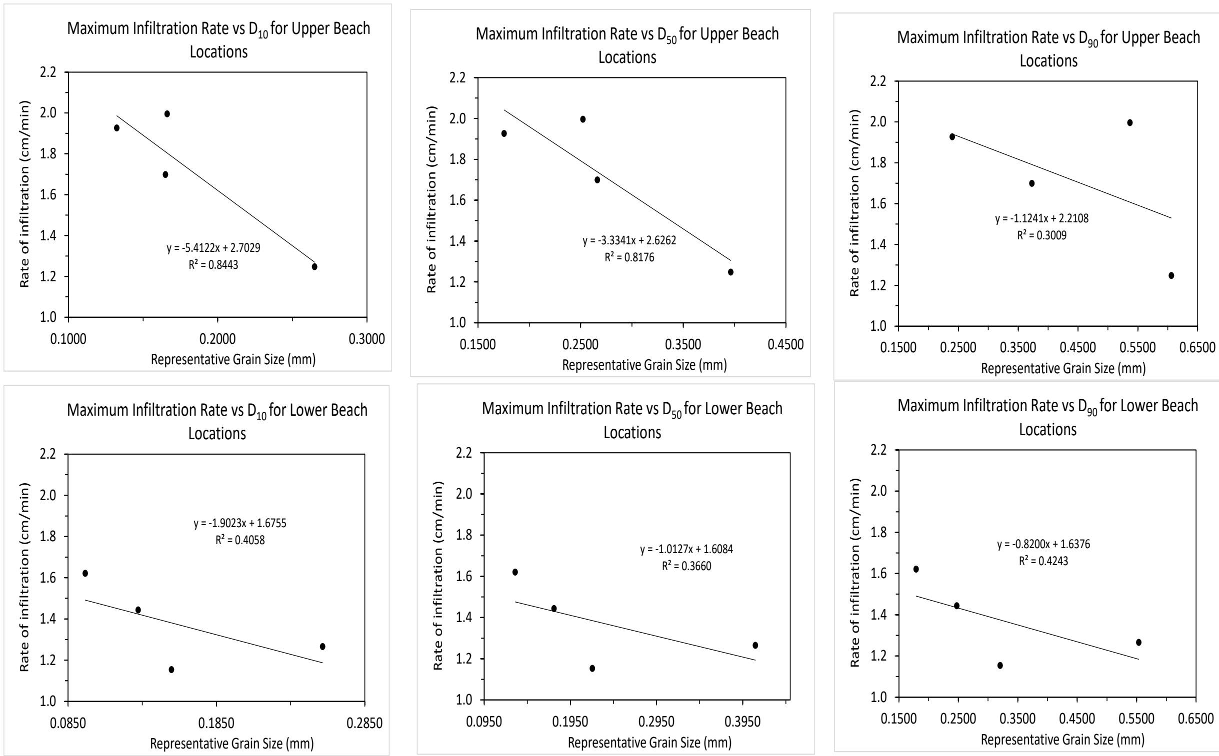

Figure 8. The Relationship between the D_{10}, D_{50}, and D_{90} Grain Sizes and the Maximum Rate of Infiltration

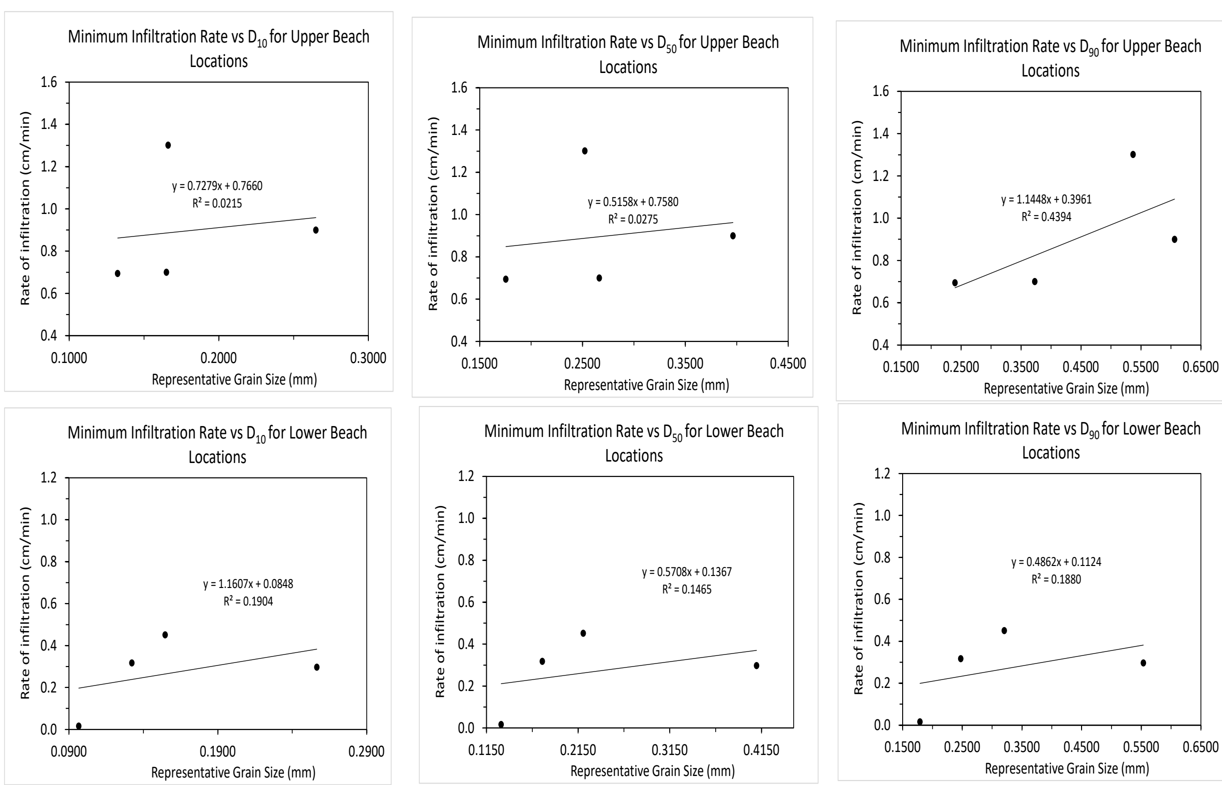

Figure 9. The Relationship between the D_{10}, D_{50}, and D_{90} Grain Sizes and the Minimum Rate of Infiltration

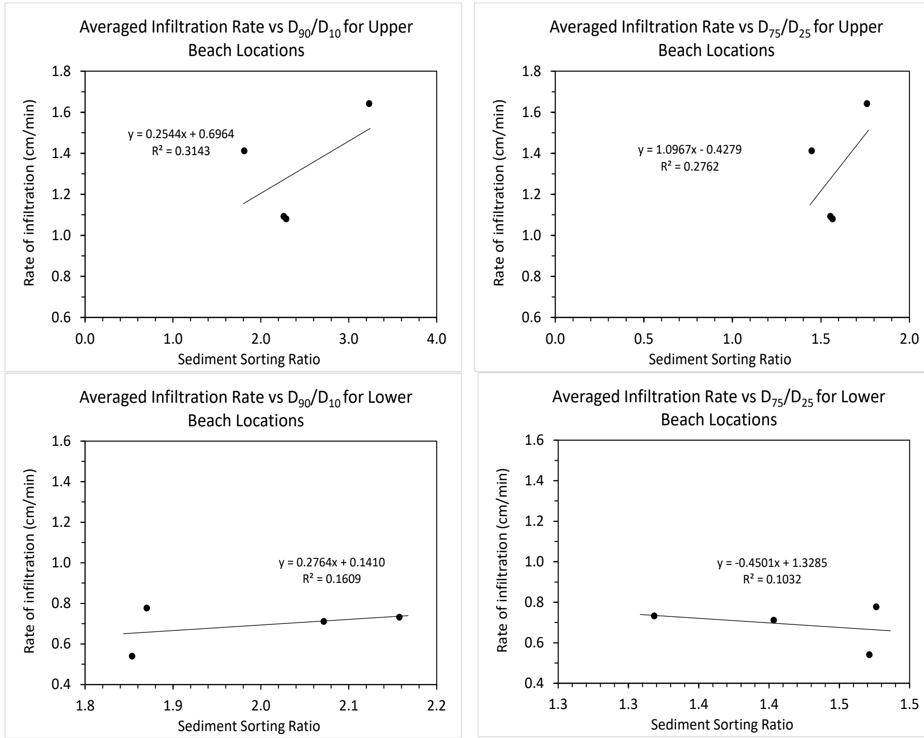

Figure 10. The relationship between the D_{90}/D_{10} and D_{75}/D_{25} Sediment Sorting Ratios and the Average Rate of Infiltration

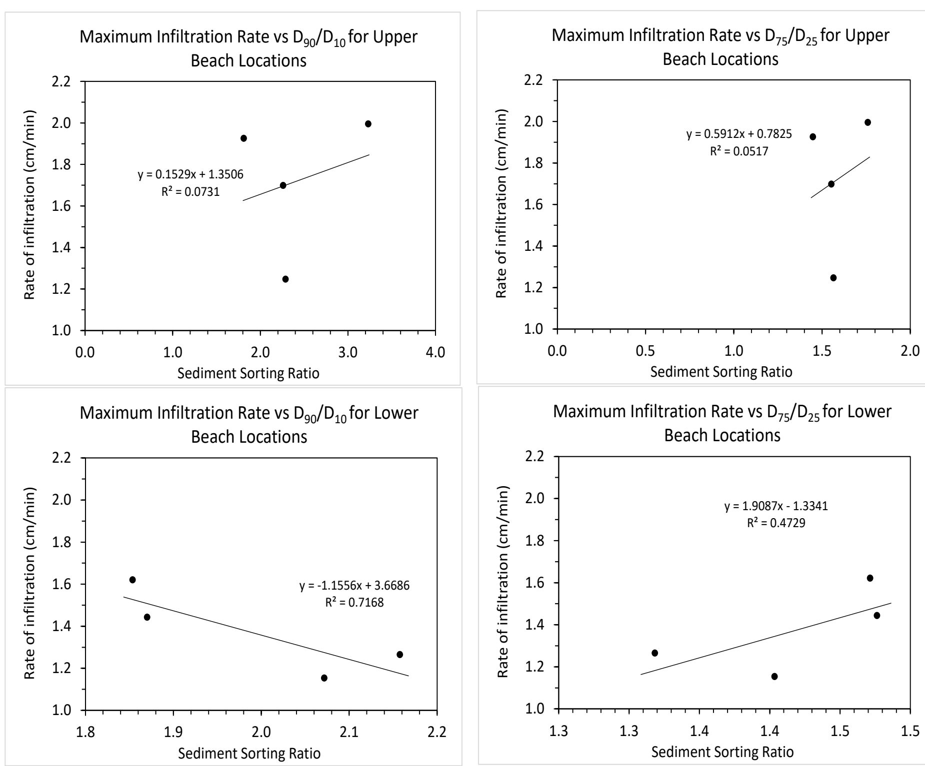

Figure 11. The Relationship between the D_{90}/D_{10} and D_{75}/D_{25} Sediment Sorting Ratios and the Maximum Rate of Infiltration

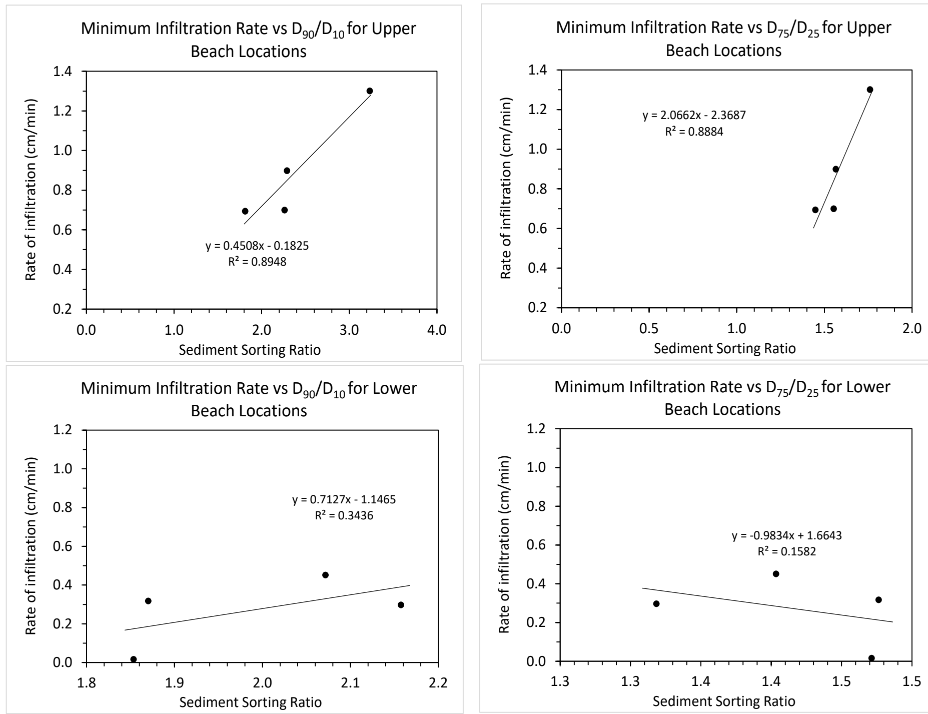

Figure 12. The Relationship between the D_{90}/D_{10} and D_{75}/D_{25} Sediment Sorting Ratios and the Minimum Rate of Infiltration

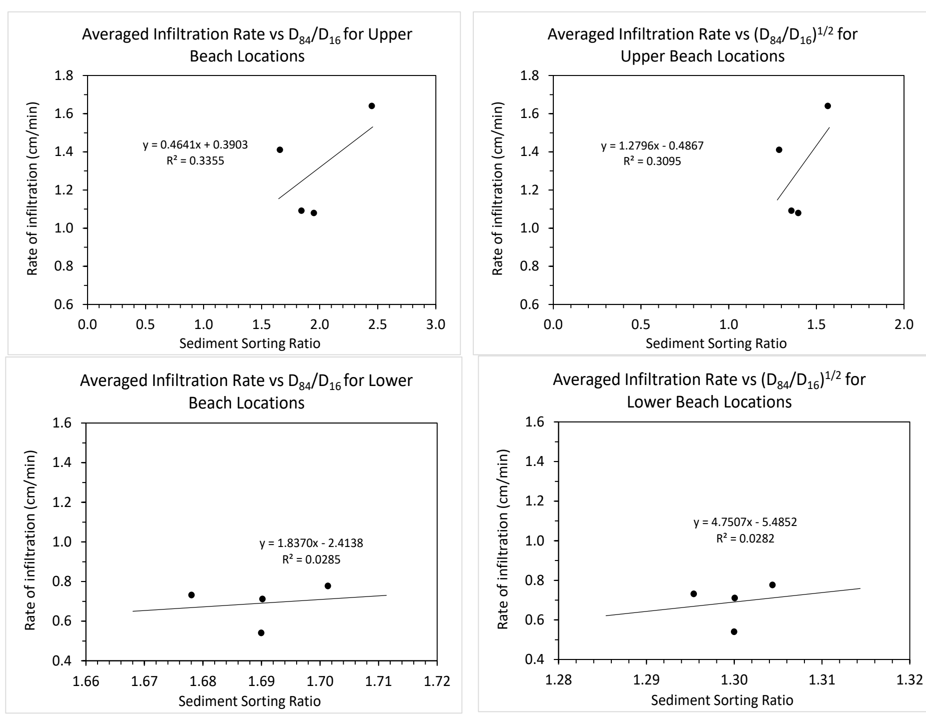

Figure 13. The Relationship between the D_{84}/D_{16} and $(D_{84}/D_{16})^{1/2}$ Sediment Sorting Ratios and the Average Rate of Infiltration

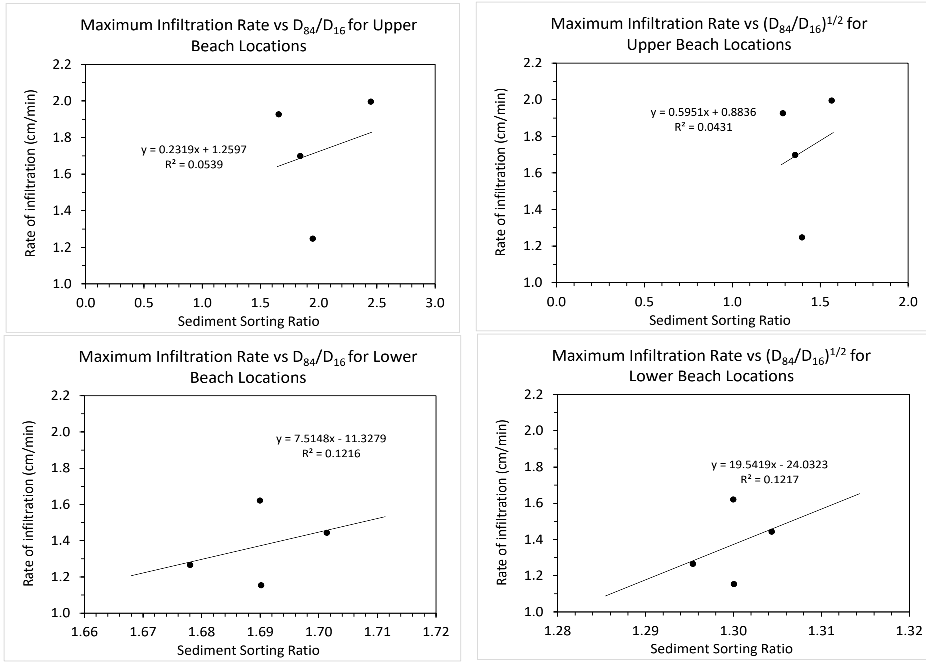

Figure 14. The Relationship between the D_{84}/D_{16} and $(D_{84}/D_{16})^{1/2}$ Sediment Sorting Ratios and the Maximum Rate of Infiltration

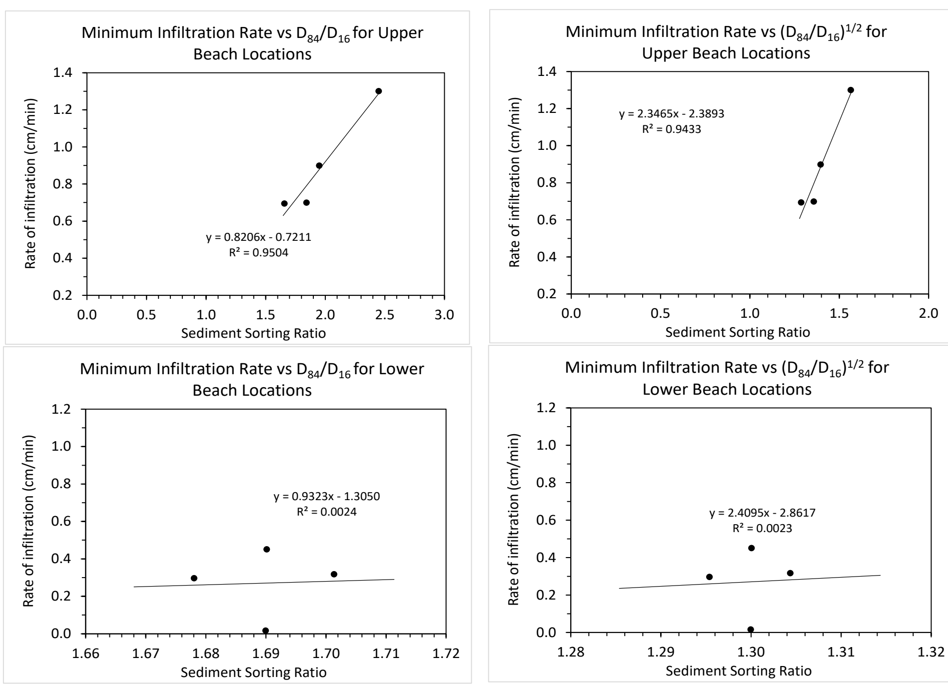

Figure 15. The Relationship between the D_{84}/D_{16} and $(D_{84}/D_{16})^{1/2}$ Sediment Sorting Ratios and the Minimum Rate of Infiltration

Authors' Biographical Notes:

Shani Brathwaite *is a graduate of The University of the West Indies, St. Augustine and is currently in pursuit of her PhD in Civil Engineering with a focus in coastal engineering. Her research interests centre on swash infiltration as an influence of the vertical positions of wave run-up.*

Deborah Villarroel-Lamb *is a Lecturer in the Department of Civil and Environmental Engineering at The University of the West Indies, St. Augustine. She specializes in coastal engineering, which includes ocean hydrodynamics, coastal morphology and coastal engineering solution.* ■